Luis Valiño[1]
Radu Mustata[1]
Juan Hierro[2]
Juan L. Hernández[3]
Martin Busack[3]
Maria J. García[3]
Carlos Blasco[3]

[1]LIFTEC/CSIC-Universidad de Zaragoza, Zaragoza, Spain.

[2]Centro Universitario de la Defensa, Zaragoza, Spain.

[3]Robert Bosch España Gasoline Systems, Aranjuez, Madrid, Spain.

3D Simulation of the Filtration and Dust Retention Process of a Fuel Filter

A model for the description of the dust retention process inside a filter was developed and successfully applied to a detailed 3D numerical simulation of a Bosch automotive diesel filter. Specifically, the variation of the pressure drop due to the clogging process in the filter paper could be well predicted. For this approach, an Eulerian-Eulerian two-phase flow formulation was applied. For the dispersed phase, the Eulerian description was made by means of a probability density function transport equation. The simulations also provide complete spatial information about the flow both in the clean and dirty sides of the filter and the particle distribution, size, and velocity. The intention of the newly developed numerical tool is to help in the design of filtering devices.

Keywords: Diesel fuel, Filtration, Fluid dynamics, Two-phase flow

Received: October 21, 2014; *revised:* March 20, 2015; *accepted:* May 20, 2015

DOI: 10.1002/ceat.201400615

1 Introduction

The cleanliness requirements of fuel injection systems are progressively demanding, according to the increasing precision required in modern automotive engines. In addition, these high cleanliness levels have to be reached for any kind of fuel found in the market. The initial dirtiness of these available fuels may span one order of magnitude, as well as their typical particle size distribution, which makes it almost impossible to define standard filters for all markets. Therefore, filter manufacturers need a broad, well-customized filter portfolio in order to provide the best filter option for each customer and market. The consequence is that a substantial number of new filters should be designed and eventually made available to production each year.

Nowadays, any engineering design requires a well-balanced succession of computational simulation and experimental results in order to reduce the time needed to obtain a proper prototype. As computers increase their power and lower their price, the role of numerical simulations is becoming predominant, for both time- and price-saving considerations. In those numerical simulations there are specific targets to achieve. These are the predictions of magnitudes which summarize the quality of the product which is being developed. In the case of a filtering device, as collected in various ISO norms, these magnitudes are the pressure drop (lifetime) and particle collection efficiency [3–5].

A numerical simulation tool with its mathematical description is presented for a given filtering device which is capable of predicting with good accuracy the lifetime of the device, taking into account the clogging of the filter and the subsequent changes both in the permeability of the filtering media and the fuel flow.

The simulation tool was created using a finite volume-based open source numerical computational fluid dynamics (CFD) code, namely OpenFOAM [6]. The particle retention model was developed and validated for simple geometries and thereafter full 3D simulations of a filtering device were carried out with good comparisons to experimental data.

2 Eulerian-Eulerian PDF Approach

In an earlier work [1], a suitable Eulerian-Eulerian formulation for the two-phase flow in the filtering device was introduced. Specifically, an Eulerian probability density function (PDF) [1, 2] is used to describe the evolution of the magnitudes associated to the disperse phase (velocity and size). The use of the PDF is justified for a laminar flow, as the one found in the studied filtering system, by the stochastic boundary conditions. In the present case, the exact velocity and position of each particle is not exactly known at the entrance, but only in a probabilistic sense. On the other hand, as this PDF has the local correlation information of those magnitudes, the velocity of the particles can be directly expressed in terms of their radius, with no need of any closure. This implies that drag and buoyancy, the main physical relevant forces acting upon the particles, can be represented locally in an exact way. The particle radius remains fixed and the Eulerian velocity is the only relevant magnitude changing in the particle, although depending on the local particle radius. The formulation is purely Eulerian, hence, the usual discretization and numerical algorithms can be applied, in opposition to Eulerian-Lagrangian formulations.

Correspondence: Prof. Luis Valiño (valino@litec.csic.es), LIFTEC/CSIC-Universidad de Zaragoza, María de Luna 10, 50018, Zaragoza, Spain.

The mathematical description can be found in the previous reference. The resulting transport equations are, however, quite intuitive and reproduced here. First, a continuity-like equation to express the conservation of the number density for the particles of each radius (there is no agglomeration or wear of the particles):

$$\frac{\partial n(r,x,t)}{\partial t} = -\frac{\partial}{\partial x_j}\left[u_j^p(r,\mathbf{x},t)n\right] \tag{1}$$

where $n(r,\mathbf{x},t)$[1)] is the expected number of particles of size r, and $u^p(r,\mathbf{x},t)$ denotes their corresponding velocity. Second, the corresponding momentum conservation, which adopts the form of the evolution of the velocity of small spherical particles in a laminar flow, considering only the dominant, drag and buoyancy, terms [7]:

$$\begin{aligned}&(\rho^p + 0.5\rho)\frac{4\pi r^3}{3}\frac{d\mathbf{u}^p}{dt} = (\rho - \rho^p)\frac{4\pi r^3}{3}\\ &\mathbf{g} - 3\rho\pi r\nu(\mathbf{u}^p - \mathbf{u}) - \frac{9\rho\pi r^2}{4}\parallel \mathbf{u}^p - \mathbf{u} \parallel (\mathbf{u}^p - \mathbf{u})\end{aligned} \tag{2}$$

where ρ^p and ρ are the densities of the particle and the fluid, respectively, $4\pi r^3/3$ is the volume of a spherical particle with diameter r, ν is the kinematic viscosity, $\mathbf{u}$ is the fluid velocity, and d/dt stands for the total time derivative of the velocity of the particle, i.e., its total acceleration, its Lagrangian time derivative. In Eq. (2), the left term represents the linear momentum variation of a spherical particle and its added mass, because of the equivalent volume of fluid which moves with the particle, whereas in the right side there is first a buoyancy contribution and, next, the drag contribution up to second order in relative velocities, i.e., velocity of the particle relative to velocity of the fluid, with an approximation valid for velocity particles whose Reynolds number based on relative velocity is less than 1, the theoretically seen drag.

The boundary conditions at the entry are given by the expected density number for each size following a prescribed log-normal PDF, equally distributed in space and assuming the particles have the local fluid velocity at the domain entry. At the exit, zero gradient conditions are used and non-slipping conditions at walls. Notice that the void fraction information is known from $n(r,\mathbf{x},t)$.

2.1 Fluid Flow Model

In diesel filtration devices for the automotive industry, the fraction of total volume occupied by particles is extremely small, so both the particle-particle interaction and the influence of the particles on the diesel flow can be neglected. However, the diesel flow cannot be solved once and for all as the progressive clogging causes an increasing pressure drop across the filter, which obviously changes the flow of diesel. Fortunately, this process is quasi-stationary, i.e., the rate of change of permeability caused by the clogging is much slower than all the other timescales of the fluid. This means that the flow can be recalculated, up to a steady state, at a finite number of times, in practice order 10, depending on flow and particle conditions along the filter lifetime.

The Navier-Stokes equation (Eq. (3)) is applied to model the flow in the pure fluid region whereas the Darcy-Brinkman equation (Eq. (4)) is employed in the porous region. It is reminded that since the evolution of the permeability is very slow in comparison to the typical flow time scales, a quasi-stationary approximation for the computation of the flow makes sense.

The resulting equations are:

$$\frac{\partial u_i u_j}{\partial x_j} = -\frac{1}{\rho}\frac{\partial P}{\partial x_i} + \frac{\partial}{\partial x_k}\left(\nu\frac{\partial u_i}{\partial x_k}\right) \tag{3}$$

$$\frac{1}{\varepsilon^2}\frac{\partial u_i u_j}{\partial x_j} = -\frac{1}{\rho}\frac{\partial P}{\partial x_i} + \frac{\partial}{\partial x_k}\left(\frac{\nu}{\varepsilon}\frac{\partial u_i}{\partial x_k}\right) - \frac{\nu}{K}u_i \tag{4}$$

where P is the fluid pressure, ε is the porosity, being the empty volume fraction available for the fluid, and K is Darcy's permeability with units of $[L]^2$. The flow is assumed to be incompressible and with constant density, i.e., the null divergence constraint is applied on the velocity field, $\nabla\,\mathbf{u} = u_{i,i} = 0$.

The previous equations are valid in porous and fluid media, assuming that in the free zones $\varepsilon = 1$ and $K = \infty$. The singularity at the interface between free and porous media is treated as in [1].

2.2 Particle Clogging Model

In order to calculate the pressure drop along the device filter, some information should be provided about the nature of the paper used as filter media and its interaction with the clogging particles absorbed. For this purpose, it is better to describe the pressure drop not directly as a function of the media permeability, but as a function of four key parameters of the filter.

2.2.1 Clean Filter

The first two parameters are the mean filter clean fiber diameter d_f and the ratio of the volume of fibers to the total filter volume, i.e., the packing density $\alpha = 1 - \varepsilon$ where ε is the porosity. These two parameters describe, through Davies' law, the pressure drop evolution of a clean fibrous filter with filtration velocity U_0 as:

$$\frac{\Delta P}{L} = 64\mu U_0\frac{\alpha^{3/2}(1 + 56\alpha^3)}{d_f^2} \tag{5}$$

where μ is the fluid dynamic viscosity and L means the thickness of the filter.

1) List of symbols at the end of the paper.

2.2.2 Clogged Filter

The other two parameters are related to the absorption process. The first one is another characteristic diameter, d_p, associated to the deposited particles, which form dendrites similar to a new collection of fibers, and finally, α_p, which is the local ratio of the volume of collected particles to the volume of the filter and is the only one which varies with time. Models like the ones by Bergman et al. [8] and Thomas et al. [9] are based on these parameters.

Herein, a model is proposed which assumes absorption of particles proportional to the local particle concentration value inside the filter, and an absorption coefficient b_p which could depend on particle size. For a (quasi-)stationary situation, with a uniform velocity distribution, normal to the paper, and an averaged absorption coefficient $b = \overline{b_p}$ for all particles, which gives the efficiency of the filter, the model would read:

$$\alpha_p(Z,t) = \frac{bX_p}{\rho_p}\frac{Q}{S}t\exp\left(-bZ\right) \tag{6}$$

where Z is the local filter depth, Q is the flow rate, S is the filtering surface, and X_p is the local mass particle concentration. The value of α_p increases with time and decreases with local depth Z in direction normal to the paper. The permeability of the medium will decrease in the opposite direction and be related to the mass of particles absorbed. Notice that $X_p \exp(-bZ)$ is the local concentration at depth Z.

A new model has been developed in this work to predict the pressure drop evolution:

$$\Delta P[t] = \frac{\mu}{S}Q\int_0^L C_1\left(1+C_2\alpha_p(Z,t)\right)^2 \left[1+\left(C_3\alpha_p(Z,t)\right)^3\right]\mathrm{d}Z \tag{7}$$

where C_1, C_2, and C_3 are unknown functions of α, d_f, and d_p whose values are to be fitted from experiments for each particular combination of filtering media and dust. Eq. (7) is a modified version of Bergman's model, but applied to a slice [8, 9]. This formula stays valid for each time increment and enables the prediction of the pressure drop during clogging.

3 Experiments and Numerical Procedure

3.1 Model Calibration

In order to calibrate the filtering media properties, a series of experiments in a simple geometrical configuration are needed. Therefore, a set of measurements of lifetime for the disk geometry of the filtering media have been performed, following the norm ISO-TR-13353. The test fluid was ShellFluid 41 doped with fine test dust A2 ISO 12103-1.

A total of three different cases were studied, and their characteristics, namely flow rate Q, filtering surface S, mass dust concentration X_p, and dust particle density ρ_p are summarized in Tab. 1.

Table 1. Parameters of the disk experiments.

	Disk 1	Disk 2	Disk 3
Q [L h^{-1}]	15	15	25
S [m^2]	0.0133	0.0133	0.0133
X_p [mg L^{-1}]	30	100	30
ρ^p [kg m^{-3}]	2650	2650	2650

The filtering media (paper) properties are presented in Tab. 2, namely thickness L, maximum pore diameter A_M, mean pore diameter A, porosity ε, and initial (clean media) permeability K_0.

Table 2. Properties of the filtering paper.

L [m]	A_M [m]	A [m]	ε	K_0 [m^2]
6.5×10^{-4}	15×10^{-6}	5×10^{-6}	0.517	2.813×10^{-13}

Following the ISO norm, the flow rate was kept constant, with the exception of the first 30 min of the test when, in order to check the efficiency of the filtering media, the dust concentration is lowered to 5 mg L^{-1}. After that period, the concentrations are given in Tab. 1. Singular pressure losses, i.e., those caused by the experimental device without the filtering element, are also taken into account.

The single fitting of Eq. (7), integrated along the filter depth L, to the experimental data for the disk configuration is excellent as it can be seen in Fig. 1.

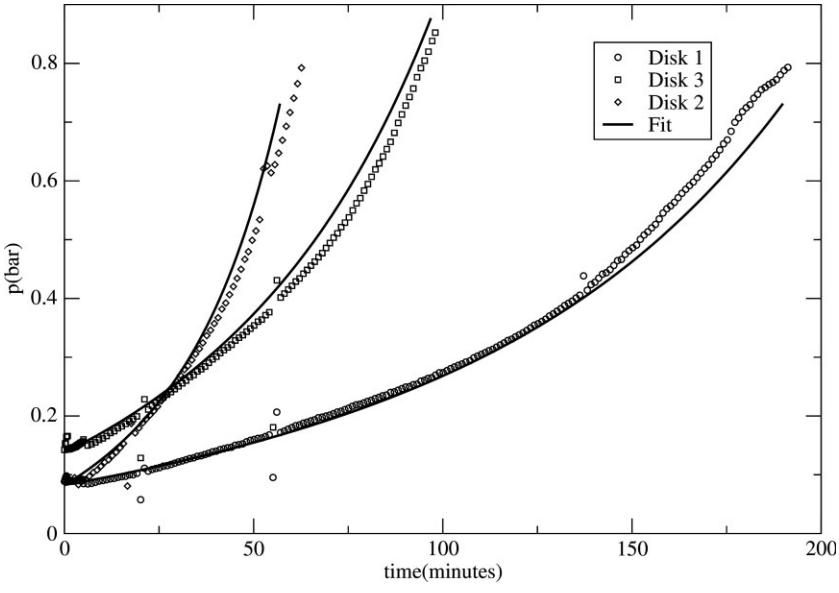

Figure 1. Pressure drop as a function of time for the three disk configurations of Tab. 1.

The progressive pressure drop in the filter device is now described by means of the same constant values of C_1, C_2, and C_3 which are presented in Tab. 3. Using specific values of the absorption coefficient b as a function of the particle size does not lead to significant improvements of the fit. Notice that specific values of b are readily obtained from efficiency experiments.

Table 3. Fitting parameters for Disk 1, 2, and 3.

C_1	C_2	C_3	b
4.06219×10^{10}	22.4152	6.92728	4096

3.2 3D Simulation

A typical filtering element is depicted in Fig. 2 a. Such a design of a filtering element is based on three geometrical parameters, namely, the filtering paper thickness L, the total filtering surface A, and the required maximum height of the filtering element H. With these three parameters, the geometrical design will result in the filtering element having a certain number of pleats, separating the, what would be, clean and dirty sides of the filter. From the numerical simulation point of view, for a detailed full 3D model a reasonable mesh would have at least a number of cells of the order presented in Fig. 2 b, namely, 3–3 M cells. As previously mentioned, the flow is quasi-stationary which means that the flow varies so slowly due to the small pressure drop rate that the flow field should be only updated for a certain number of times during the lifetime simulation. If one is seeking for reasonable computing times, this process inevitably requires a further simplification of the geometry of study down to a "building block", and in the current case this could be considered the geometry of a single pleat, with a certain height and with a filtering paper of certain thickness.

In all that follows, 3D simulation results will be presented for a single pleat geometry, with a mesh size of around 70K cells, as depicted in Fig. 3. A block-structured mesh was generated using the in-code mesher of OpenFOAM for this geometry. The model of particle retention was implemented in a custom solver [1] for filtering developed as a module in OpenFOAM.

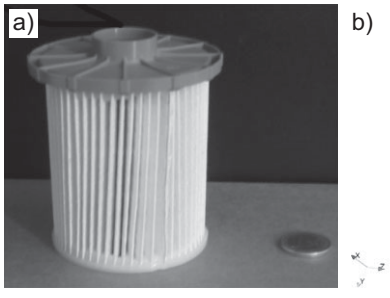

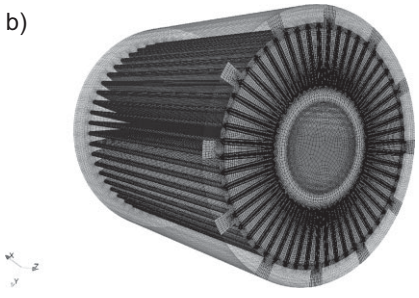

Figure 2. (a) Bosch filter device with the external wall removed to see the filtering paper. The flow enters vertically through the upperside external slots and exits through the upperside central duct. (b) 3.3M cell mesh.

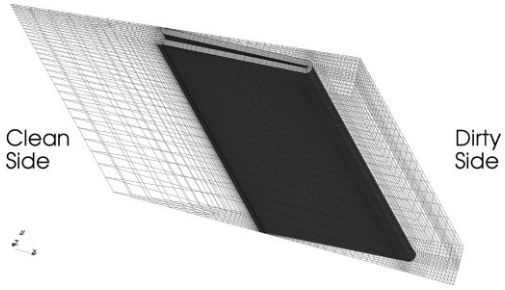

Figure 3. 3D 70K cell, one pleat mesh.

Two cases are presented here with inflow fluid rates of 120 and 210 L h^{-1} doped with fine test dust A2-fine of concentration $X_p = 50$ mg L^{-1}.

Detailed flow and particle topology in a more realistic geometry, namely one-sixth of the filtering element in Fig. 2 b was described in [1] for a clean filter situation. It could be seen that the flow field and the particle concentrations were no longer uniform across the filter surface. Therefore, the direct use of Eq. (7) considering the same parameters, i.e., filtering area, flow rate, and particle concentration, is expected not to produce reasonable results which can be observed in Fig. 4.

For a 3D configuration, Eq. (7) should be applied locally in space. This approach is valid because, as it can be seen in Fig. 5, in almost every zone of the filter, the velocity vectors of the flow are normal to the entry/exit surface. The small differences occur where the pleat bends are not expected to produce significant errors in the model.

In Fig. 6, the pressure drop through the filter and the velocity vectors are presented both in a state that corresponds to the first update of the flow field during clogging (a) and the final one (b) where the pressure drop reaches the limiting value prescribed in the ISO-TR-13353 lifetime norm. Notice that the flow pattern is not very dissimilar. The pressure drop takes place mostly in the filtering media. However, there are, as expected, changes in the way the clogging process affects the pressure drop across the filtering media.

Fig. 7 a demonstrates that the inner corners of the pleat in the clean side become firstly affected by the particle clogging, thus, making the pressure drop progressively faster in that area. With time, those areas practically do not filter anymore and the model predicts qualitatively well the transition towards the straight parts of the pleat where most of the filtration takes place during the lifetime of the device.

The variations in permeability across the filtering paper width are presented in Fig. 6 as a result of applying the model of Eq. (7) locally. The progressive permeability loss in the first layers of the filtering media facing the dirty side of the filter and normal to the flow direction will cause the pressure drop to be confined to these areas; see Figs. 7 b and 6 b.

The 3D simulations do not give only a qualitative match to the experiments, but also a quantitative one and in terms of comparisons with the experiments a considerable improvement is achieved.

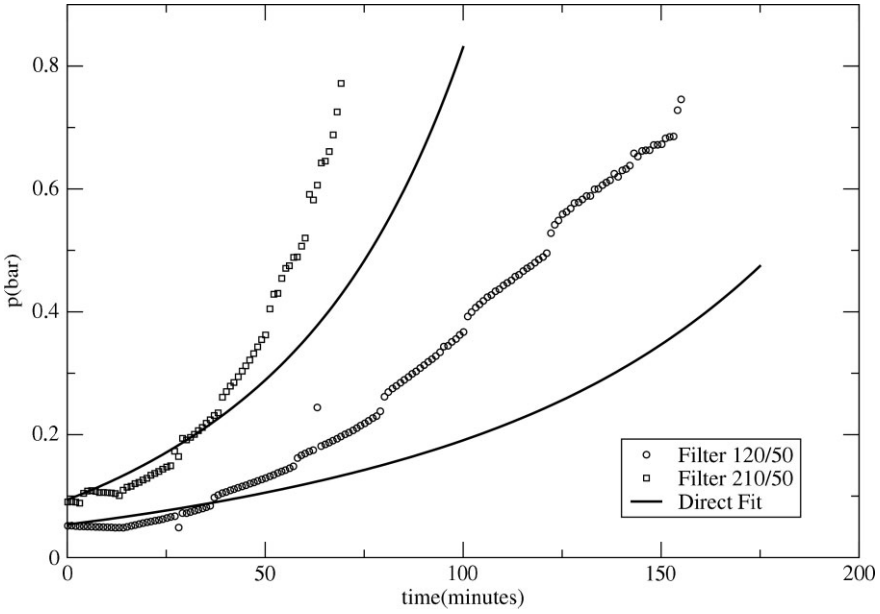

Figure 4. Pressure drop as a function of time for a 3D filter model using Eq. (7).

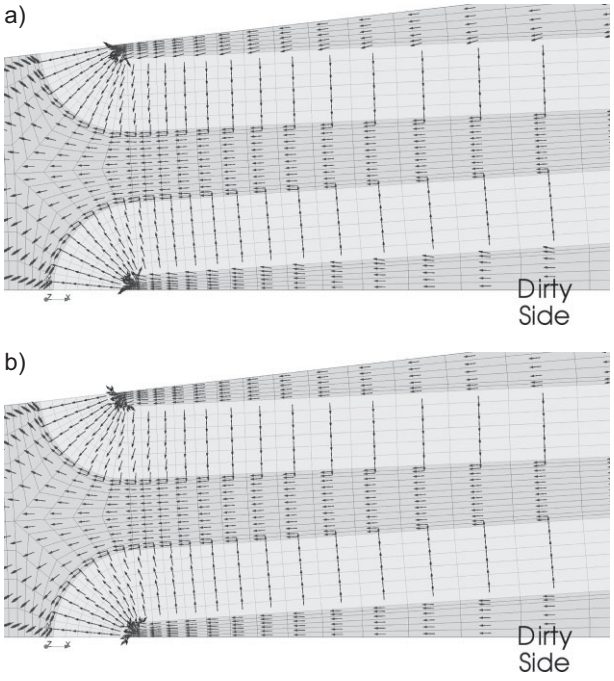

Figure 5. View of velocity vectors on a mesh cut at midheight plane of the model: (a) initial state, (b) final state.

This is reflected in the lifetime prediction as presented in Fig. 8. Not only the lifetime value, which is the ultimate goal of the simulation, but also the intermediate pressure loss due to the clogging process is much better compared with the experimental data.

4 Conclusions

Simulations of a particle filtering inside an automotive filter have been presented to model the lifetime in detail of a standard Bosch automotive filter device.

For the distribution of particle retention, including size effects, the continuous phase governing equations are supplemented with transport equations for the particle size distribution, using a PDF formalism combined with an absorption law for particles, size-dependent, and a pressure drop model expressing the effect of clogging. Both the absorption law and the pressure model have been developed to characterize the filter paper properties regarding particle retention, for a specific paper and dust composition. Being able to fit three different flows for the same paper and dust composition confirms the robustness of the approach.

Once the characteristic parameters are fitted for a given filtering paper and test dust in a simplified configuration, the progressive effects of the non-homogeneous permeability induced by the retention of particles is studied in a standard Bosch filter device for the same filtering paper and dust. A good agreement can be noticed between the model and the experiments, proving the feasibility of this approach. The numerical simulations of the proposed equations have been carried out using an in-house modulus for filtering, developed on top of OpenFOAM.

Acknowledgment

This work was supported by the Spanish Government through the PCA10 project.

The authors have declared no conflict of interest.

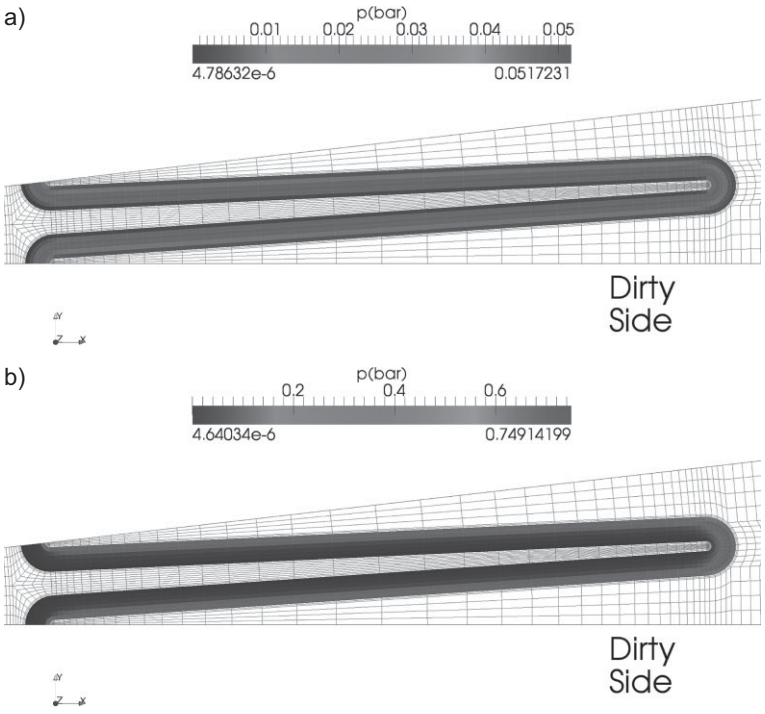

Figure 6. View of the pressure map on a mesh cut at midheight plane of the model: (a) initial state, (b) final state.

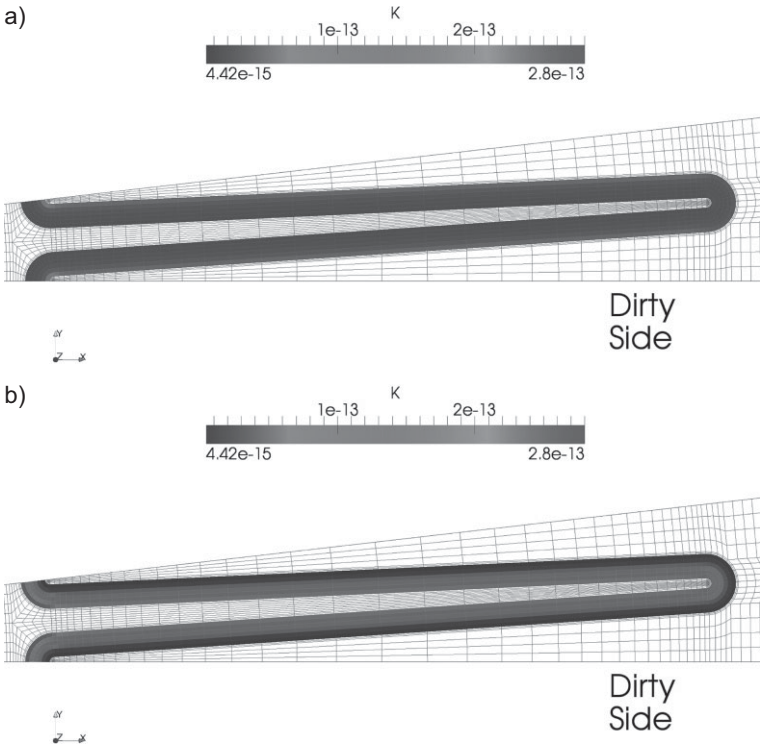

Figure 7. View of the permeability map on a mesh cut at midheight plane of the model: (a) initial state, (b) final state.

Symbols used

$A(m)$	[m]	mean pore diameter
$A_M(m)$	[m]	maximum pore diameter
b_p	[–]	filter absorption coefficient depending on particle size
b	[–]	size-averaged filter absorption coefficient
C_1, C_2, C_3	[–]	parameters of the pressure drop model
d_f	[m]	mean filter clean fiber diameter
d_p	[m]	characteristic diameter associated to the deposited particles
K	[m^2]	Darcy's permeability
K_0	[m^2]	initial (clean) permeability
L	[m]	thickness of the filter
P	[bar]	diesel pressure
Q	[$L\,h^{-1}$]	flow rate
$(r,\mathbf{x},t)$	[–]	dependency on size r, position $\mathbf{x}$, and time t
S	[m^2]	filtering surface
$\mathbf{u}$	[$m\,s^{-1}$]	diesel velocity
$\mathbf{u}^p$	[$m\,s^{-1}$]	particle velocity
U_0	[$m\,s^{-1}$]	filtration velocity
v	[$m^2\,s^{-1}$]	kinematic viscosity of diesel
X_p	[$mg\,L^{-1}$]	local mass particle concentration
Z	[m]	spatial coordinate through the filter thickness

Greek letters

α_p	[–]	local ratio of the volume of collected particles to the volume of the filter
α	[–]	packing density, i.e., ratio of the volume of fibers to the total filter volume
ε	[–]	porosity, i.e., the empty volume fraction available for the fluid
μ	[$kg\,m^{-1}\,s^{-1}$]	dynamic viscosity of diesel
ρ^p	[$kg\,m^{-3}$]	particle density
ρ	[$kg\,m^{-3}$]	diesel density

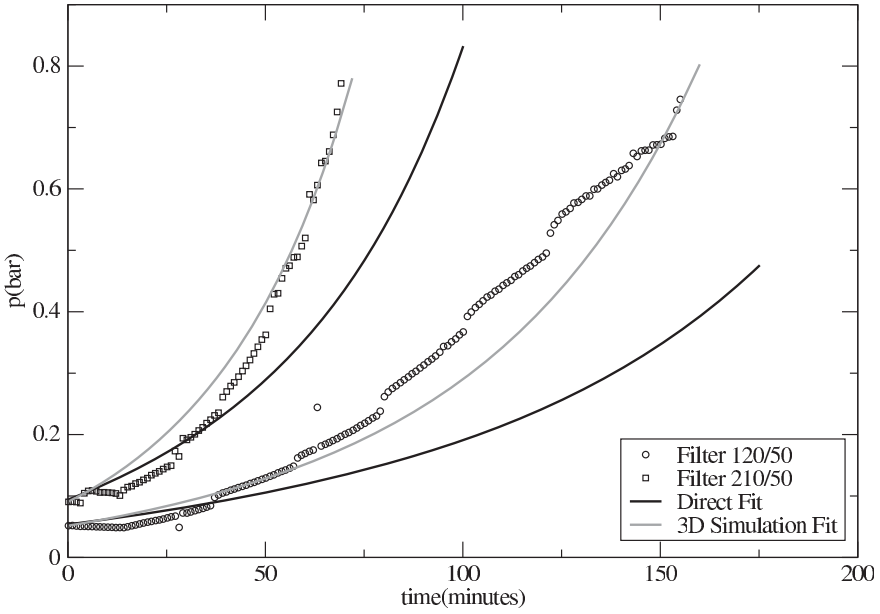

Figure 8. Lifetime prediction for the simplified 3D geometry of one pleat.

References

[1] L. Valiño, R. Mustata, J. Hierro, J. L. Hernández, C. Blasco, *Proceedings FILTECH*, Wiesbaden, October **2009**.

[2] L. Valiño, *Flow Turbul. Combust.* **1998**, *60*, 157–172.

[3] F. Gruschwitz, H. Nirschl, H. Anlauf, *Chem. Eng. Technol.* **2014**, *37 (6)*, 1043–1048.

[4] P. C. Gervais, N. Bardin-Monnier, D. Thomas, *Chem. Eng. Sci.* **2012**, *73*, 239–248.

[5] S. Fotovati, H. Vahedi Tafreshi, P. Pourdeyhimi, *Sep. Purif. Technol.* **2012**, *98*, 344–355.

[6] OpenCFD Ltd. (ESI Group), http://www.openfoam.com, **2014**.

[7] E. Loth, *Prog. Energy Combust. Sci.* **2009**, *26*, 161–223.

[8] W. Bergman, R. D. Taylor, H. H. Miller, *15th DOE Nuclear Air Cleaning Conference*, CONF-780819, Boston, MA, August **1978**.

[9] D. Thomas, P. Penicot, P. Contal, D. Leclerc, J. Vendel, *Chem. Eng. Sci.* **2001**, *56*, 3549–3561.